EVAPORATION

IN A COASTAL SUBARCTIC WETLAND

DURING THE GROWING SEASON

BY

PETER DAVID BLANKEN

A Research Paper

Submitted to the Department of Geography

in Fulfilment of the Requirements

of Geography 4C6

McMaster University

Hamilton, Ontario, Canada

April 1990

ABSTRACT

Energy balance components were measured over a coastal subarctic wetland in northwestern James Bay during the growing season. The Penman-Monteith combination model was used to determine surface and atmospheric controls on evaporation. The Priestley-Taylor combination model was used to calculate an evaporability parameter, α. Combining these two models resulted in determining the sensitivity of α to surface and atmospheric controls.

Canopy, aerodynamic, and climatological resistances were influenced by onshore or offshore wind directions. Canopy resistance was dominant and showed a strong seasonal trend. α averaged 0.78 and was influenced by wind direction. α is most sensitive to canopy resistance, followed by vapour pressure deficit, net available energy, and aerodynamic resistance.

ACKNOWLEDGEMENT

The author would like to thank the supervisor of this thesis, Dr. W. R. Rouse, for always having time for suggestions, comments, and discussions concerning this topic.

TABLE OF CONTENTS

LIST OF TABLES

LIST OF FIGURES

CHAPTER 1 - INTRODUCTION

1.1 Research Objectives

This paper studies the boundary layer climate of a coastal subarctic wetland in northwestern James Bay. It particularly focuses on the process of evaporation. Evaporation is an important process because it is the connecting link between the climatic and the hydrologic cycles. Evaporation is important ecologically since most plants rely on the movement of water through their roots systems and stomatal cells in order to make use of soil nutrients. It also plays an important role in the prediction of future climates. If evaporation is increased as a result of a warmer climate, the warming trend may be amplified since water vapour, as a greenhouse gas, is an efficient absorber of long wave radiation. This is discussed in detail by Raval and Ramanathan (1989) and Manabe and Wetherald (1967).

The first objective of this paper is to determine the factors which limit the evaporation process. The second is to determine the value of an evaporability parameter α. The third is to determine the sensitivity of α.

In pursuing the three objectives stated above, the data are divided into onshore or offshore wind directions. The purpose of this is to determine how advection affects

the evaporation process. Throughout this paper, evaporation, evapotranspiration, and the latent heat flux (Qe) terms are used synonymously. SI (Système International) units are used throughout.

1.2 Review of the Penman-Monteith Model

The original empirical method for determining evaporation was to treat the process as a function of vertical vapour pressure gradients and a coefficient of turbulent mixing. An alternative to this method was to regard the process as a function of the energy balance at the Earth's surface. Penman (1948) combined these two approaches, eliminating the need to measure surface temperature which was a difficult variable to measure. Penman applied his derived equation to successfully model evaporation from open water.

Building on Penman's work, Monteith (1965) attempted to reconcile climatological concepts of evaporation with the physiological controls on evaporation exerted by vegetation. In doing so, Monteith added terms to Penman's equation which account for the regulatory control of the water vapour flux exerted by leaves. This leaf control is accomplished by the stomata which regulate the exchange of gases between the plant and atmosphere (Arms and Camp, 1982). This model became known as the Penman-Monteith combination model for

evaporation and is given by

$$Qe = \frac{S(Q^* - Qg) + \rho Cp[e_s(T_a) - e_a]/r_a}{S + \gamma(1 + r_c/r_a)} \qquad (1)$$

where S is the slope of the saturation vapour pressure versus temperature curve; Q* is the net all wave radiation; Qg is the subsurface heat flux; ρ is the density of air; Cp is the specific heat of air at constant temperature; e_s is the saturation vapour pressure; T_a is the ambient air temperature; e_a is the ambient vapour pressure; r_a is the aerodynamic resistance; γ is the psychrometric constant and; r_c is the canopy resistance.

This one-dimensional model is termed a `combination´ model since it combines aerodynamic and energy balance theory. Also, the model is combinational since both available energy and moisture are incorporated. McNaughton and Jarvis (1983) describe the applications of the model to different types of vegetation, and Lafleur and Rouse (1988) discuss the application of the model to different surfaces in a coastal zone of the subarctic.

1.3 Review of Resistances

The exchange of gases between a surface and the atmosphere can be understood using the electrical analogue defined by Ohm´s Law. This states that the flow of current in an

electrical circuit is equal to the electrical potential (voltage) divided by the wire resistance. Similarly, the flux of gases is equal to the concentration difference of the gas divided by the resistance to flow exerted by the system (Oke, 1978). This resistance represents a measure of how the system inhibits the flow of gases to the atmosphere. In this paper, water vapour is the only gas that is considered. The resistances that are considered are canopy, aerodynamic, and climatological.

The climatological resistance is calculated using the Bowen ratio (β) given by

$$\beta = \frac{Qh}{Qe} = \gamma \frac{\Delta T_a}{\Delta e_a} \qquad (2)$$

where Qh is the sensible heat flux. The partitioning of energy at the surface is given by

$$Q* = Qh + Qe + Qg \qquad (3)$$

Combining equations (2) and (3) gives the Bowen Ratio Energy Balance (BREB) equation

$$Qe = \frac{(Q* - Qg)}{(1 + \beta)} \qquad (4)$$

Combining equations (1) and (4) and solving for β yields

$$\beta = \frac{r_c + r_a - r_i}{[S/\gamma]\, r_a + r_a} \qquad (5)$$

where r_i is the climatological resistance given by

$$r_i = \frac{\rho Cp}{\gamma} \quad \frac{e_s(T_a) - e_a}{Q* - Qg} \qquad (6)$$

A large r_i indicates that evaporation is enhanced, not inhibited. Lafleur and Rouse (1988) reported that r_i varied little between three contiguous wetland surfaces of alder/willow woodland, sedge marsh, and sedge meadow located in a subarctic coastal marsh. r_i, however, varied markedly with wind direction (table 1).

The canopy resistance is determined by measurements of the stomatal resistance and the leaf area index using the relationship $r_c = r_{st} \times LAI$, where r_{st} is the bulk surface resistance and LAI is the leaf area index. When measurements of r_{st} and LAI are not available, r_c can be determined by calculating the bulk surface resistance given by

$$r_c \approx r_{st} = (\beta + 1)r_i + [\beta(S/\gamma) - 1] \qquad (7)$$

Lafleur and Rouse (1988) state that site differences in r_{st} were directly related to the biophysical properties of the vegetation canopies. For example, the LAI for the woodland site was approximately twice as large as the other sites which resulted in a smaller r_{st} value. Table 1 gives representative r_c values for different vegetation.

The aerodynamic resistance for momentum is calculated using the wind speed measured at a single level and parameters determined by the aerodynamic characteristics

of the canopy (Thom, 1975). The aerodynamic resistance is determined using

$$r_a = \frac{[\ln(z - D)/z_0]^2}{k^2 u_z} + r_b \qquad (8)$$

where u is the wind speed at height z; D is the zero-plane displacement; z_0 is the surface roughness length; k is von Karmen's constant and; r_b is a correction factor used to account for excessive resistance to heat and vapour incurred by bluff body forces (Lafleur and Rouse, 1988). As suggested by Thom (1975), $r_b = 4/u*$ where u* is the frictional velocity.

Lafleur and Rouse (1988) reported that r_a was consistently smallest at the woodland site because of the large surface roughness length (table 1). r_a values for the sedge marsh and sedge meadow site were similar because of the similar canopy morphologies. The authors note that wind speed did not change with wind direction, hence r_a varied little with wind direction.

1.4 Review of the Evaporability Parameter α

Priestley and Taylor (1972), while investigating the partitioning between sensible heat and evaporation, developed a special form of the combination equation of evaporation. This model, known as the Priestley-Taylor

model, is given by

$$Qe = \alpha[S/(S + \gamma)](Q^* - Qg) \qquad (9)$$

where α is an evaporability parameter relating actual to potential evaporation. Solving equation (9) for α gives

$$\alpha = \frac{Qe}{[S/(S + \gamma)](Q^* - Qg)} \qquad (10)$$

When α is equal to unity, the model gives the equilibrium evaporation. Using equation (9), Priestley and Taylor (1972) found that for a variety of surfaces with an unlimited water supply, an α value of 1.26 was appropriate.

Rouse et al. (1977), while investigating the application of the model, reported that α decreased from 1.26 (potential conditions) to 0.97 and 0.91 for a old and new burn lichen woodland, respectively. This decrease is likely due to available soil moisture. For a wet sedge meadow, α equalled 1.26 since the surfaces were continuously wet. For upland lichen heath, α = 0.95 and soil moisture played no role because of the overwhelming control exerted by the thick lichen mat.

An investigation into the effects of Hudson and James Bays on the coastal energy balance by Rouse et al. (1986) included the calculation of α. The authors report that α values are smaller during cold onshore winds than warm offshore winds.

Bello and Smith (1990) report on the behaviour of α over a lake in the Hudson Bay Lowlands. Their results show that local advection is primarily responsible for large latent heat fluxes. Although α averaged 1.35 over the summer, hourly and daily values were highly variable. Most of this variability could be reconciled with changing weather conditions (i.e. sunny, cloudy, rainy, or evening conditions).

1.5 Derivation of α using the Penman-Monteith Model

To accomplish the third objective, the value of Qe which appears in the numerator of equation (10) is that obtained by the Penman-Monteith combination model. Combining equations (1) and (10) gives

$$\alpha = \frac{S(Q^* - Qg)(S + \gamma) + S\rho CpVPD/r_a + \gamma\rho CpVPD/r_a}{S(Q^* - Qg)(S + \gamma) + S(Q^* - Qg)\gamma r_c/r_a} \qquad (11)$$

where VPD is the vapour pressure deficit. Figure 1 shows that the Penman-Monteith estimate of Qe is insensitive to all but very small values of r_a. Within the range of r_a measured in this study, Qe using the BREB approach and Qe using the Penman-Monteith approach gave a 1:1 relationship with $r^2 = 0.99$. Therefore, equation (11) is valid for this study.

CHAPTER 2 - STUDY SITE

2.1 Site Location

The study site (figure 2) is located on the western coast of James Bay, 20 km north of the mouth of the Ekwan River and just north of Ekwan Point (53°17´N, 82°07´W).

The coastal topography is very flat with an elevation rise inland of 0.2 %. The region is rapidly rising due to isostatic rebound in response to the removal of the Wisconsin ice sheet some 10,000 years ago (Sugden and John, 1985). This process has resulted in a series of well-developed raised beaches extending inland from the coast. This coastal zone marks the southern limit of continuous permafrost and the northern limit of the tree line, since both converge at approximately 53°N (Rouse et al., 1987).

2.2 Vegetation

As noted by Kadonaga (1989), distinct vegetation zones are evident at Ekwan Point. In general, fens have developed in the poorly-drained depressions, while the upland raised beaches are dominated by small shrubs, stunted trees, and lichens.

The vegetation nearest the main climate site consisted of *Potentilla egedii* and *Carex subspathacea*. Soils

in the area consisted of beach soils with deposits of sand and gavel evident to a depth of at least 0.30 m.

CHAPTER 3 - METHODOLOGY

3.1 Instrumentation

The main measurement site was located in an open coastal area, approximately 575 m from the mean high water mark (figure 2). Q* was measured with an aspirated Middleton net pyrradiometer. Qg was measured with a Middleton heat flow transducer. See Halliwell and Rouse (1988) for details on methods used to correct the underestimate of Qg typically made by heat flow transducers. Temperature and vapour pressure gradients were measured with shielded psychrometers mounted at 0.5, 1.0, 1.5, and 2.0 m above the surface. Each psychrometer contained two thermocouples, one dry and one wet, with water supplied by a reservoir via a saturated cotton wick. The psychrometers were aspirated by battery powered fans.

Wind speed was measured with Young 3-cup analogue output anemometers located on a separate mast at heights of 0.5, 1.0, 1.5, and 2.0 m above the surface. Wind direction was determined by a Young wind vane positioned on top of the wind mast.

Signals from the instruments described above were recorded on a Campbell Scientific CR-7 data logger with a scan interval of 10 seconds. Values were integrated every 60 minutes, then averaged for the entire day. The measurement period began on June 29, 1988 and ended on August 3, 1988.

3.2 Wind Direction Division

Initial analysis involved dividing the data into either onshore or offshore wind direction. The coast runs north-south (figure 2), therefore winds blowing from the east have originated over James Bay, and are termed onshore winds. Conversely, winds blowing from the west have originated over the land surface, and are termed offshore winds. The term `allwinds' refers to winds blowing from any direction (average conditions for the entire measurement period). Of the 35 day measurement period, 23 experienced onshore winds, and 12 experienced offshore winds.

CHAPTER 4 - RESULTS

4.1 General Climate

Climate records for a 29 year period were compared to the observed measurements for the month of July. The closest long-term records available are at Moosonee, Ontario, which

is located approximately 250 km SSE of Ekwan Point. Table 2 gives climate normals (where normal refers to the 29 year average at Moosonee) and a summary of boundary layer climate recorded at the study site.

The environments over which the onshore and offshore winds originate are distinct. James Bay is relatively shallow (46 m maximum) which increases the duration of sea ice cover well into the growing season. In late June, 75 % of James Bay has from 20 - 80 % ice cover. This decreases to 50 % of the Bay having between 10 - 50 % ice cover in early July. In late July and early August, a further decrease of 25 % of the Bay having between 10 - 20 % ice cover occurs (Danielson, 1969). As a consequence of this long duration of ice cover, sea surface temperatures range from 7 - 11 °C in July to 8 - 14 °C in August (Danielson, 1969).

In contrast, the land surface's river ice has broken by May 20, with lake ice persisting until June 1 (Hutton and Black, 1975). Mean monthly surface air temperatures range from 7 - 13 °C in June, 13 - 18 °C in July and, 10 - 16 °C in August (Danielson, 1969).

4.2 Seasonal Patterns

Figure 3 shows a time series of evaporation and precipitation. The evaporation time series shows a seasonal

trend, reaching a minimum value on Julian Day 198 (July 17). The precipitation plot shows that rainfall was sparse, occurring only 34 % of the days.

4.3 Resistances

Table 3 gives resistance values. The canopy resistance, r_c, was 6 s/m larger for offshore than onshore winds. Note that r_c is, on average, approximately four times r_a. The aerodynamic resistance, r_a, was 14 s/m larger for onshore than offshore winds. Also, the range of r_a was 58 s/m larger for onshore than offshore wind directions. Unlike r_a and r_c, the climatological resistance, r_i, for onshore and offshore winds was very different (table 3c). r_i was more than 2.5 times for offshore winds and the range of values was more than twice as great. Figure 4 shows a time series of all three resistances. It shows that all resistances have a large daily variability.

Figure 3c focuses on the time series of r_c. The three-day running mean indicates a strong seasonal trend with r_c peaking around Julian Day 200 (July 19). This seasonal trend shows the effects of high Qe and small rainfall as the growing season progresses.

4.4 Evaporability Parameter

Table 4 shows the results obtained using the Priestley-Taylor model of evaporation when solved for α (equation 10). Average values for α are small compared to α = 1.26. For offshore winds, α is 0.19 larger than for onshore winds. Also, the range of α is 0.34 larger for offshore winds.

4.5 Sensitivity of α to Atmospheric and Surface Controls

The ranges and average values of the variables that appear in equation (11) are given in table 5. Figure 5 shows that α decreases exponentially as r_c increases. Sensitivity is greatest for small r_c and offshore wind conditions. For example, an increase in r_c from 100 to 300 s/m results in a 0.2 and 0.4 increase in α for onshore and offshore winds, respectively. Offshore α values are always greater than onshore α values for the ranges encounter during the measurement period. Figure 6 indicates a clear linear relationship between α and VPD. This can be approximated by the equation α = 0.58(VPD) + 0.40. Wind direction has no significant effect on this relationship. Figure 7 shows that α decreases exponentially as Q* - Qg increases. The sensitivity of α to Q* - Qg decreases as Q* - Qg becomes large. α is more sensitive to offshore than onshore wind conditions. Offshore values of α are consistently larger

than onshore values. Figure 8 shows the sensitivity of α to r_c. Contrary to expectations, α increases as r_a increases. Note that wind direction changes the magnitude but not the sensitivity of α to r_c. α is 0.25 greater for offshore than onshore winds.

Table 6 summarizes the order of sensitivity of α to each of the variables. Overall, α is more sensitive to offshore wind conditions. The range of α for a variable r_c, VPD, and $Q^* - Q_g$ increases by 58 %, 56 %, and 48 %, respectively, during offshore winds. The range of α for a variable r_a decreases by 67 % during offshore winds.

CHAPTER 5 - DISCUSSION

5.1 Resistances

The canopy resistance is a composite measure of surface dryness and stomatal resistance. The large values of r_c indicate that surface was very dry. Figure 3 reveals that this drying trend increased as the growing season progressed. Before Julian Day 200 (July 19), the small rainfall (figure 3a) causes the surface to dry out and the stomatal resistance to increases. In response, evapotranspiration decreased as the canopy resistance increased. After Julian Day 200, rainfall events provided

water allowing the surface to dampen and stomatal resistance to decrease. Evapotranspiration then began to increase as the canopy resistance decreased. Note that figures 3b and 3c are mirror images.

The daily variation of r_c is related more to stomatal resistance than surface dryness. Stomatal behaviour is influenced by light, air or leaf temperature, humidity, water status, and CO_2 concentration (Lafleur, 1988). A general response of stomata is to increases resistance as the VPD increases. McNaughton and Jarvis (1983) report that this response has been found for as many as 200 plant species. Lafleur and Rouse (1988) reported that in a subarctic coastal marsh, large r_{st} values occurring with offshore winds (table 1) were probably a result of the stomatal response to the increasing VPD. In this study, the offshore average VPD = 0.6 kPa, and the onshore average VPD = 0.3 kPa. Based on the stomatal response to VPD, the average offshore r_{st} should be much greater than the average onshore r_{st}. Table 3a shows that this did not occur. It is likely that the stomata are responding to a combination of the influences described above.

The aerodynamic resistance is affected by plant morphology, wind speed, and surface roughness. The zero-plane displacement, D, (equation 8) gives a quantitative

estimate of the role of plant morphology in determining r_i. D is related to the height of the vegetation, and is a function of the shape and density distribution of the leaves (Oke, 1978). As plant height increases, r_i will decrease (with a constant wind speed). In this experiment, the sedge grass grew 0.10 m during the measurement period. An increase of 0.10 m in plant height corresponds to an 16 s/m decrease in r_i if all other variables are held constant. This trend, however, does not appear in a time series of r_a (figure 4). Therefore plant induced wind roughness does not seem to affect r_i, presumably because the LAI is so small.

r_a was larger during onshore than offshore winds (table 3b). Figure 9 shows that as wind speed increases, r_a decreases exponentially. Since the difference between average onshore and offshore wind speed in not significant (onshore = 4.6 m/s; offshore = 5.2 m/s), wind speed does not account for the differences in r_i values. Surface roughness coupled with tidal conditions may explain the differences in r_i values. Although tide times are not known, with onshore winds, tide-out conditions would create a large z_0 due to the exposed boulders (Silis, 1987). This would tend to decrease r_i. In contrast, onshore winds with tide-in conditions would create a small z_0 causing r_a to increase.

r_i is not a true resistance, but only conveniently

has units of resistance (Lafleur and Rouse, 1988). r_i responds to the VPD and to the available energy (equation 6). Since the available energy shows no systematic trend with time or wind direction, r_i becomes largely a function of the VPD. The large VPD values associated with offshore winds result in large r_i values. The wide range of r_i values during offshore winds is a result of the wide range of VPD values during these conditions.

The net resistance can be calculated as

$$r_{net} = r_a + r_c - r_i \qquad (12)$$

Note that r_i is subtracted from the other resistances since positive r_i values indicate that evaporation is enhanced. The higher the net resistance, the greater the evaporation is inhibited (from equation 12). During onshore winds, the value of r_{net} is 302 s/m. Offshore winds result in a r_{net} value of 240 s/m. Based on these values, evaporation should be greatest during offshore winds. This agrees with observed measurements. Average Qe calculated using the BREB approach gave an onshore value of 62 W/m^2, and a offshore value of 76 W/m^2. A simple calculation reveals that Qe increases 23 % with offshore winds, and the r_{net} increases a very similar 26 % with offshore winds. This indicates a substantial atmospheric control on Qe.

5.2 Behaviour of α

The allwinds average of $\alpha = 0.78$ is well below the $\alpha = 1.26$ which is the value commonly quoted for a continuously wet surface (Priestley and Taylor, 1972). This is expected since a coastal sedge meadow is not continuously wet. The low α value indicates that the surface was very dry. This is confirmed by high a r_c. The average values of α for precipitation and non-precipitation days are 0.98 and 0.73, respectively. This indicates that the atmosphere was close to saturation (i.e. $\alpha = 1$) during precipitation events.

An offshore wind direction had the effect of increasing α from 0.71 to 0.90 (21 %), placing evaporation close to equilibrium in the absence of advection. This implies that with offshore winds, the deficit in evaporation caused by lack of rainfall could be partially eliminated. However, since days with onshore winds (23) greatly outnumber days with offshore winds (12), this balancing will not occur.

5.3 Sensitivity of α

Figure 5 reveals that as the surface dries (large r_c), α decreases. Contrary to r_p the VPD does not overpower the effect of r_c on α. The sensitivity of α is greatest for a small r_c. This indicates that initial drying of a wet

surface will cause a sudden drop in α. Once the surface has become very dry, α becomes insensitive to changes. Since offshore winds are warm and dry, α is consistently larger during offshore winds. Note that the sensitivity of α to r_s increases during offshore winds.

A large VPD corresponds to a large α (figure 6). As the air becomes drier, α increases in a linear fashion. The sensitivity of α to VPD does not change with wind direction. Only the magnitude of α is affected by wind direction. Since offshore winds have a larger VPD than onshore winds, the value of α is also larger.

Referring to figure 7, α is large and sensitive to small values of Q* - Qg. The average Q* - Qg during days with precipitation (117 W/m2) is smaller than non-precipitation days (141 W/m2). Therefore a small Q* - Qg corresponds to periods when there is available surface moisture due to precipitation input. These conditions allow evaporation to increase, bringing the surface and atmosphere close to equilibrium.

It is expected that as r_s increases, α would decrease since evaporation is inhibited. Figure 8, however, shows that increasing r_s results in a non-linear increase in α. The increase in α is larger for a small r_s. For wind speeds less than 4 m/s, the average VPD is 0.2 kPa; greater than 4

m/s, the average VPD is 0.4 kPa. As wind speed increases, r_a decreases (figure 9) while at the same time the VPD increases, which has the effect of increasing α (figure 6). Figure 8 shows that the sensitivity of α to the VPD is greater to that of r_a. Through the common factor of wind speed, the effects of r_a and VPD on α counteract one another, with the VPD effect wining out. Offshore α's are consistently greater than onshore α values due to the large VPD associated with offshore winds.

Overall, α is most sensitive to r_c (table 6). This is because r_c is the most important indicator of the surface moisture state. The sensitivity of α to VPD ranks second indicating that VPD is the most important indicator of the atmosphere's ability to accept moisture from the surface. α's sensitivity to $Q^* - Q_g$ ranks third showing that the energy available to drive evaporation is not as important as surface or atmospheric moisture states. The sensitivity of α to r_a ranks fourth indicating that r_a plays a minor role in the evaporation process.

CHAPTER 6 - CONCLUSIONS

The Penman-Monteith combination model shows the following. The total resistance, r_{tot}, is increased by 21 % during

offshore winds. Due to a decrease in precipitation and an increase in evaporation as the growing season progressed, a strong seasonal trend was shown by r_c. A two-times increase in the VPD which occurred with offshore winds did not significantly increase r_c. A large r_a occurs with onshore winds due to a longer surface roughness length during tide-out conditions. r_a was of secondary importance for both wind directions.

The Priestley-Taylor combination model indicates the following. A calculated value of α indicated that the surface was evaporating near equilibrium with the atmosphere during rainfall events. On average, a 26 % decrease in α occurred during days with no rainfall. Warm, dry offshore winds increased α by, on average, 21 %.

The evaporability term, α, is sensitive in declining importance to r_c, VPD, $Q^* - Qg$, and r_a. These results indicated the following: 1) α decreased exponentially as r_c increased; 2) α increased linearly as VPD increased; 3) α decreased exponentially as $Q^* - Qg$ increased and; 4) α increased as r_a increased. This unusual behaviour of the sensitivity of α to r_a was due to the overpowering effect of VPD on α. The sensitivity of α is greatest with the initial drying of the surface.

Ending on an ecological note, the James Bay Power

Project, when completed, would harness 20 rivers draining 350,000 km^2 of northwestern Quebec (Gorrie, 1990). A consequence of this (not to mention numerous others) would be to reverse the natural pattern of seasonal river flow. Instead of maximum flow occurring during the spring melt, it would instead occur during the winter. This might decrease the amount of sea ice, resulting in an earlier sea ice spring melt. Rouse and Bello (1985) have empirically shown that a shift from onshore to offshore winds is likely to occur with an earlier sea ice melt in Hudson Bay. As this paper has shown, evaporation would be increased with a higher frequency of offshore winds.

The overall importance of surface and atmospheric controls on evaporation in a subarctic coastal wetland has been shown. In combination with previous studies it is evident that controls on evaporation operate everywhere from western Hudson Bay through the southern tip of James Bay. Any events which alter the overall climate, the offshore sea ice, or the vegetation in the Hudson Bay Lowlands are likely to alter the evaporation regime and the water balance in these delicate subarctic environments.

REFERENCES

Arms, K. and Camp. P. S.. 1982, `*Biology*´, Saunders, New York, 942 pp.

Bello, R. and Smith, J. D.. 1990, `The Effect of Weather Variability on the Energy Balance of a Lake in the Hudson Bay Lowlands, Canada´, *Arctic and Alpine Res.* **22**, 98-107.

Danielson, E. W.. 1969, `*The Surface Heat Budget of Hudson Bay*´, Marine Science Centre - McGill University, Montreal, 196 pp.

Environment Canada. 1982a, `*Canadian Climate Normals 1951-1980 - Volume 3. Precipitation*´, Atmospheric Environment Service, Ottawa. 602 pp.

Environment Canada. 1982b, `*Canadian Climate Normals 1951-1980 - Volume 2. Temperature*´, Atmospheric Environment Service, Ottawa. 306 pp.

Gorrie, P.. 1990, `The James Bay Power Project´, *Canadian Geographic* **110**, 20-31.

Halliwell, D. H. and Rouse, W. R.. 1987, `Soil Heat Flux in Permafrost. Characteristics and Accuracy of Measurement´, *J. Climatol.* **7**, 571-584.

Hutton, C. L. A. and Black, W. A.. 1975, `*Ontario Arctic Watershed - Map Folio No. 2*´, Mutual Press, Ottawa. 107 pp.

Kadonaga, L. K.. 1989, `Stomatal Response of Carex Aquatilis to Climate Conditions in a Subarctic Coastal Wetland During the Growing Season´, Unpublished B.Sc. thesis, McMaster University. 57 pp.

Lafleur, P.. 1988, `Leaf Conductance of Four Species Growing in a Subarctic Marsh´, *Can. J. Bot.* **66**, 1367-1375.

Lafleur, P. M. and Rouse, W. R.. 1988, `The Influence of Surface Cover and Climate on Energy Partioning and Evaporation in a Subarctic Wetland´, *Boundary-Layer Meteorol.* **44**, 327-347.

Manabe, S. and Wetherald, R.T.. 1967, `Thermal Equilibrium of the Atmosphere with a Given Distribution of Relative Humidity', *J. Atmos. Sci.* **24**, 241-259.

McNaughton, K. G. and Jarvis, T. A.. 1983, `Predicting Effects of Vegetation Changes on Transpiration and Evaporation', in T. T. Kozlowski (ed.), *Water Deficits and Plant Growth*, Academic Press, New York, pp. 2-47.

Monteith, J. L.. 1965, `Evaporation and Environment', *Symp. Soc. Exp. Biol.*, **XIX**, Cambridge University Press, London, pp. 205-234.

Oke, T. R.. 1978, `*Boundary Layer Climates*', Methuen, London, 372 pp.

Penman, H. L.. 1947, `Natural Evaporation from Open Water, Bare Soil and Grass', *Proceedings of the Royal Society* **193**, 120-145.

Priestley, C. H. S. and Taylor, R. J.. 1972, `On the Assessment of Surface Heat Flux and Evaporation Using Large-Scale Parameters', *Mon. Wea. Rev.* **100**, 81-92.

Raval, A. and Ramanathan, V..1989, `Observational Determination of the Greenhouse Effect', *Nature* **342**, 758-761.

Rouse, W. R. and Stewart, R. B.. 1972, `A Simple Model for Determining Evaporation from High-Latitude Upland Sites', *J. Appl. Meteor.* **11**, 1063-1070.

Rouse, W. R., Mills, P. F., and Stewart, R. B.. 1977, `Evaporation in High Latitudes', *Water Resour. Res.* **13**, 909-914.

Rouse, W. R. and Bello, R. L.. 1985, `Impact of Hudson Bay on the Energy Balance in Hudson Bay Lowlands and the Potential for Climatic Modification', *Atmosphere-Ocean* **23**, 375-392.

Rouse, W. R., Hardill, S. G., and Lafleur, P.. 1987, `The Energy Balance in the Coastal Environment of James Bay and Hudson Bay During the Growing Season', *J. Climatol.* **7**, 165-179.

Silis, A.. 1987,`The Energy Balance of the Intertidal Zone of Hudson Bay During the Ice-Free Summer´, Unpublished M.Sc Thesis, McMaster University. 86 pp.

Sugden, D.E. and John, B. S.. 1985, `*Glaciers and Landscapes*´, Arnold, Great Britain, 376 pp.

Thom, A. S.. 1975, `Momentum, Mass and Heat Exchange of Plant Communities´, in J. L. Monteith (ed.), *Vegetation and the Atmosphere*, Vol. 1, Academic Press, New York, pp. 57-110.

TABLES

Table 1. Comparison of resistance for different vegetation under various conditions.

	r_i	r_c	r_{st}	r_a
Lafleur and Rouse, 1988				
Sedge Marsh				
Onshore	21		48	35
Lateral	40		39	41
Offshore	90		87	36
Sedge Meadow				
Onshore	16		50	30
Lateral	37		70	36
Offshore	85		107	32
Woodland				
Onshore	22		24	11
Lateral	36		37	18
Oke, 1978				
Short Grass		70		70
Crops		40		30
Forests		125		5
Open Water				200
McNaughton and Jarvis, 1983				
Dry Forest		40-100		5-10
Dry Crop		20-60		20-200
Wet Forest		< 5		5-10
Wet Crop		< 5		20-200

Table 2. Average daily values of the boundary layer climate for the entire measurement period (appendix for symbols and units). Square brackets refer to July mean values; round brackets refer to July normal values (Environment Canada, 1982a, and Environment Canada, 1982b).

Q*	Qh	Qe	Qg	β	Kd	Ku	Alb	T_a	e_a	P	ET
143	69	69	6	1.12	265	62	0.23	12.4 [12.1] (15.3)	1.4	2.3 [79.1] (95.9)	2.3

Table 3. Values for the (A) canopy, (B) aerodynamic, and (C) climatological resistances (s/m). C.V. is the coefficient of variation of the resistances.

A

	Allwinds	Onshore	Offshore
Average	230	228	234
Minimum	51	51	55
Maximum	503	429	503
Range	452	377	448
C.V.	0.47	0.45	0.52

B

	Allwinds	Onshore	Offshore
Average	107	112	98
Minimum	41	41	66
Maximum	154	154	121
Range	113	113	55
C.V.	0.24	0.26	0.17

C

	Allwinds	Onshore	Offshore
Average	64	38	92
Minimum	13	13	37
Maximum	177	86	177
Range	164	73	139
C. V.	0.67	0.50	0.40

Table 4. Values for the evaporability parameter α.

	Allwinds	Onshore	Offshore
Average	0.78	0.71	0.90
Minimum	0.51	0.51	0.52
Maximum	1.41	1.06	1.41
Range	0.90	0.55	0.89
C.V.	0.28	0.21	0.30

Table 5. Average, minimum, and maximum values for the variables required to calculate α using the Penman-Monteith combination model of evaporation.

		Allwinds	Onshore	Offshore
r_c	Average	230	228	234
	Minimum	51	51	55
	Maximum	503	429	503
VPD	Average	0.4	0.3	0.6
	Minimum	0.1	0.1	0.3
	Maximum	1.4	0.6	1.4
Q*-Qg	Average	133	133	131
	Minimum	61	61	72
	Maximum	193	193	184
r_a	Average	107	112	98
	Minimum	41	41	66
	Maximum	154	154	121

Table 6. Order of sensitivity over full range of α over full range of r_c, VPD, $Q^* - Qg$, and r_a for offshore and onshore winds. Parenthesis indicate ranking of sensitivity.

	Offshore	Onshore
r_c	0.69 (1)	0.50 (1)
VPD	0.45 (2)	0.20 (2)
$Q^* - Qg$	0.29 (3)	0.15 (4)
r_a	0.06 (4)	0.18 (3)

FIGURES

Figure 1. Sensitivity of the Penman-Monteith estimate of Qe to r_s.

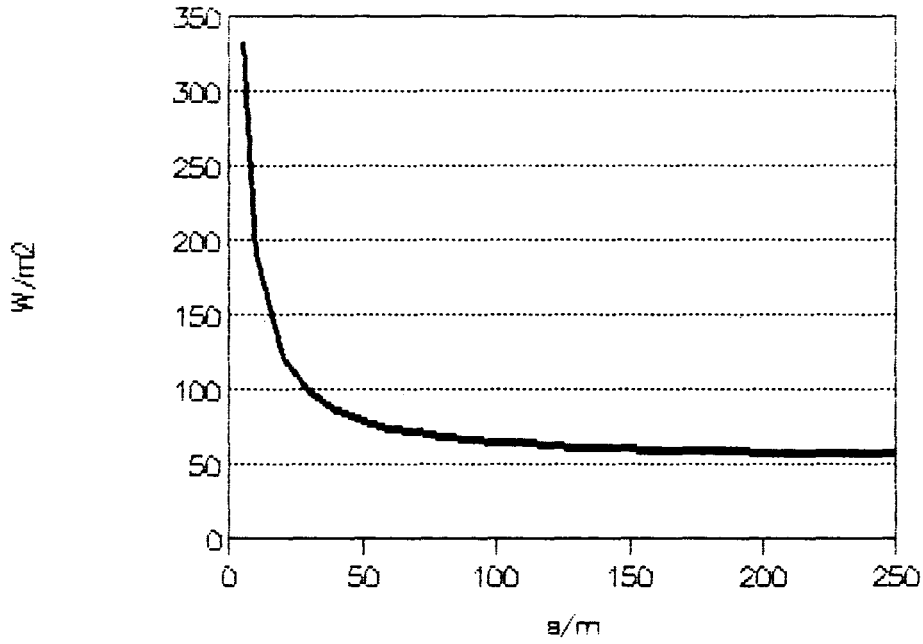

Figure 2. Location of study area. Modified from Kadonaga (1989).

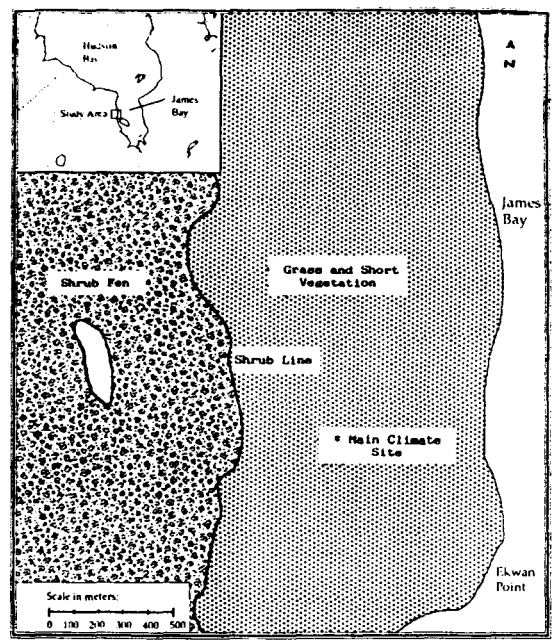

Figure 3. Seasonal patterns of (A) precipitation, (B) evapotranspiration, and (C) canopy resistance (thin line), and 3-Day running mean (thick line).

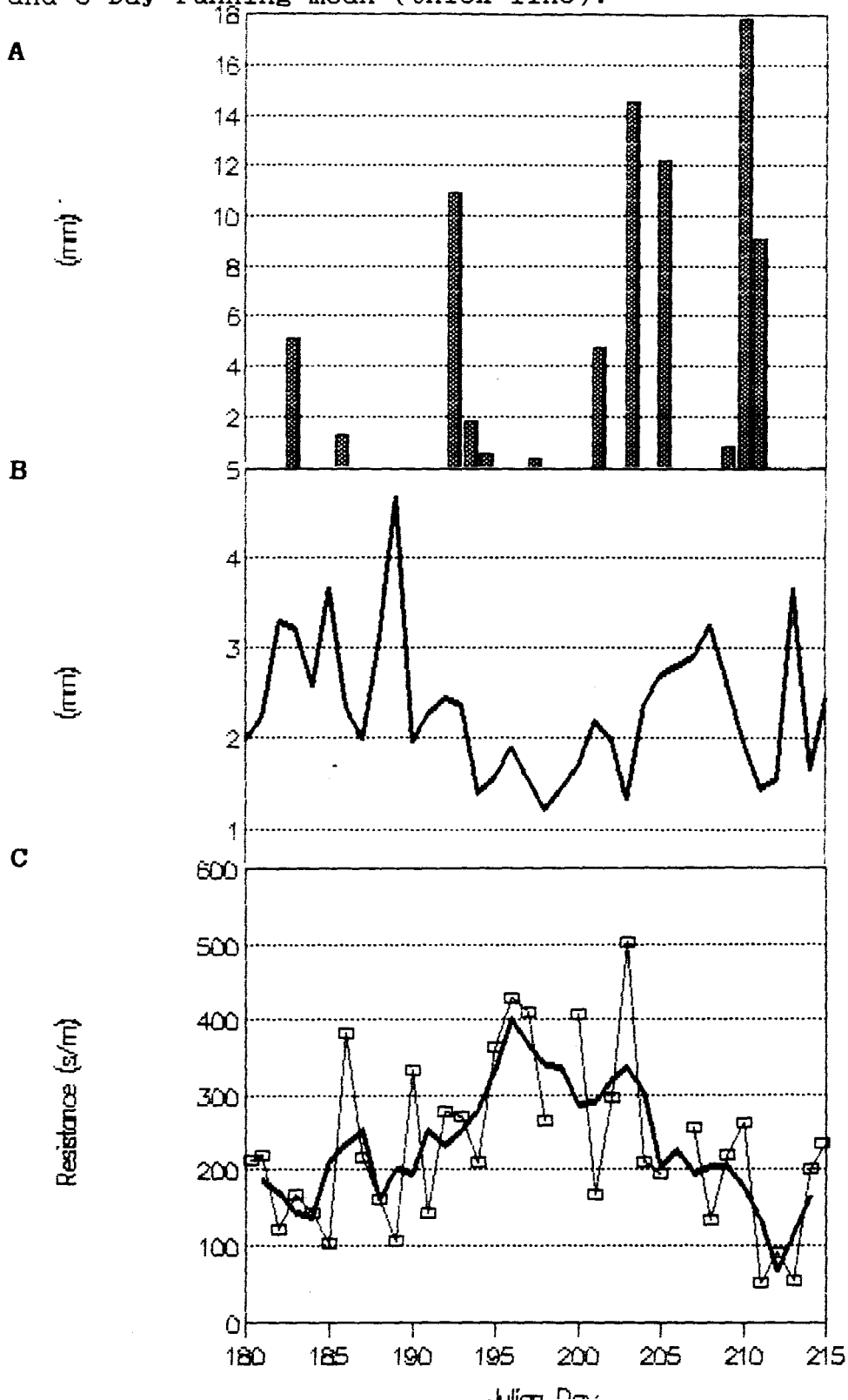

Figure 4. Seasonal patterns of canopy, aerodynamic, and climatological resistances. Julian Days 180 and 215 correspond to June 29 and August 3, respectively.

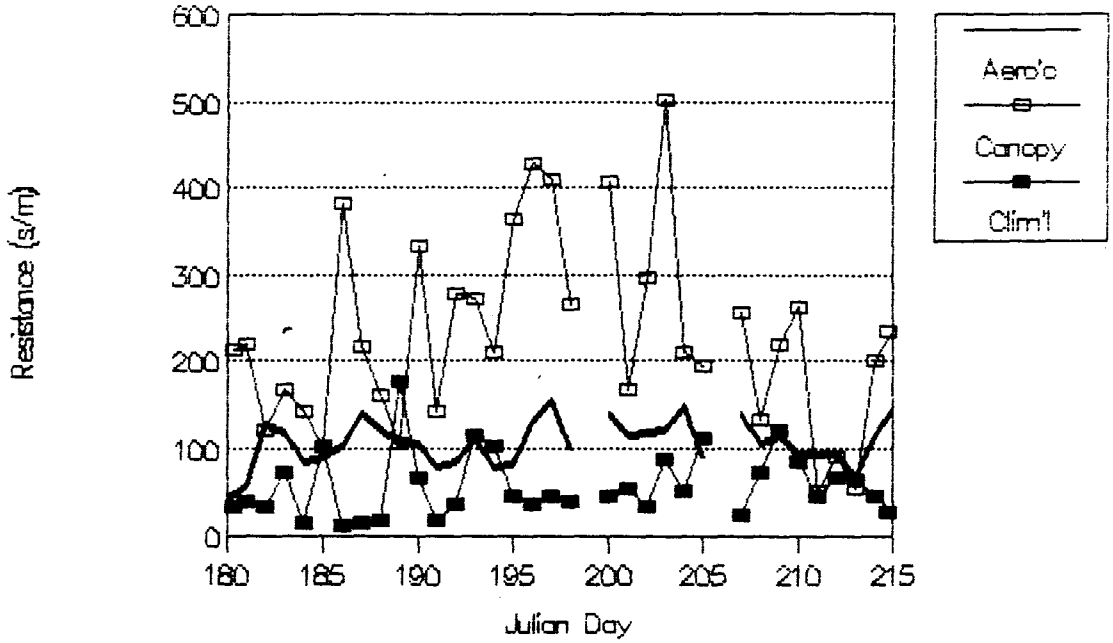

Figure 5. Sensitivity of α to r_c.

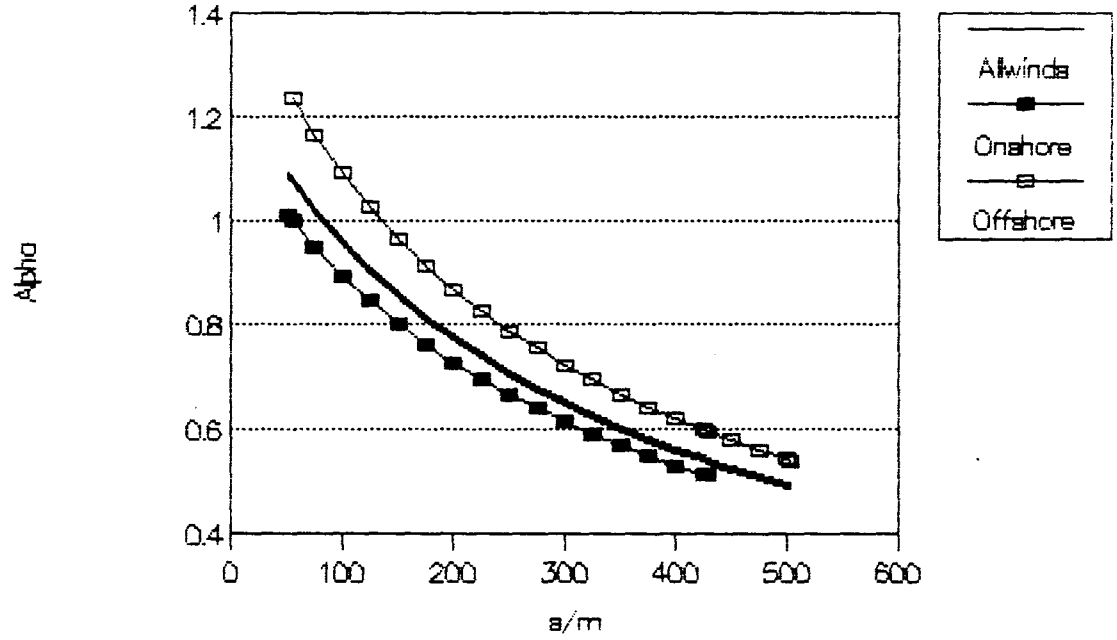

Figure 6. Sensitivity of α to VPD.

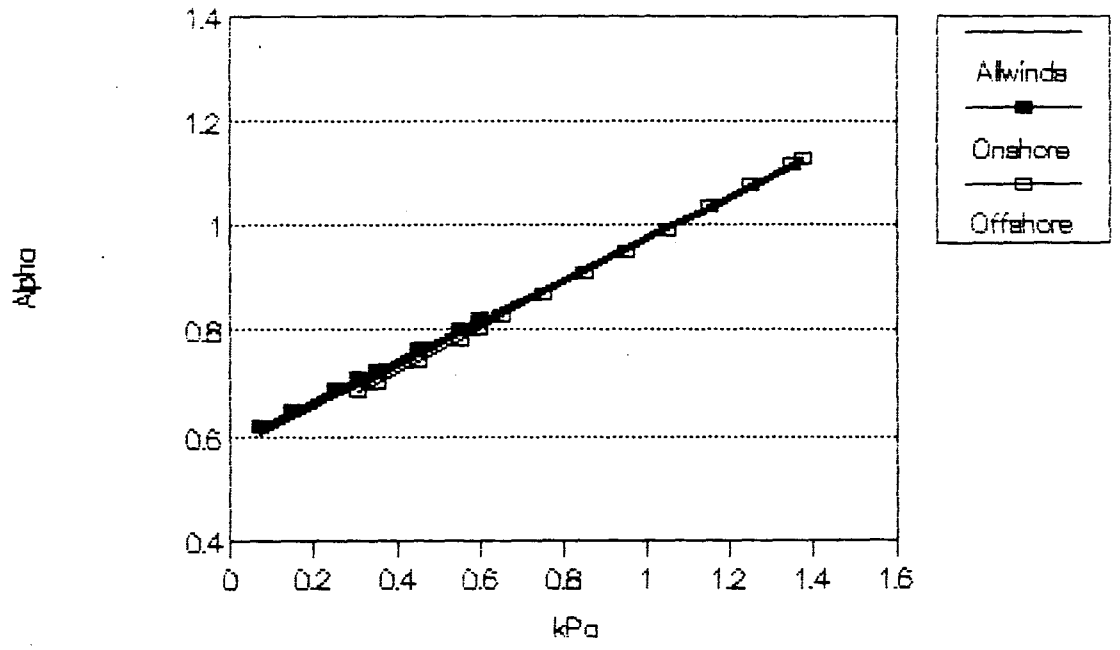

Figure 7. Sensitivity of α to Q* - Qg.

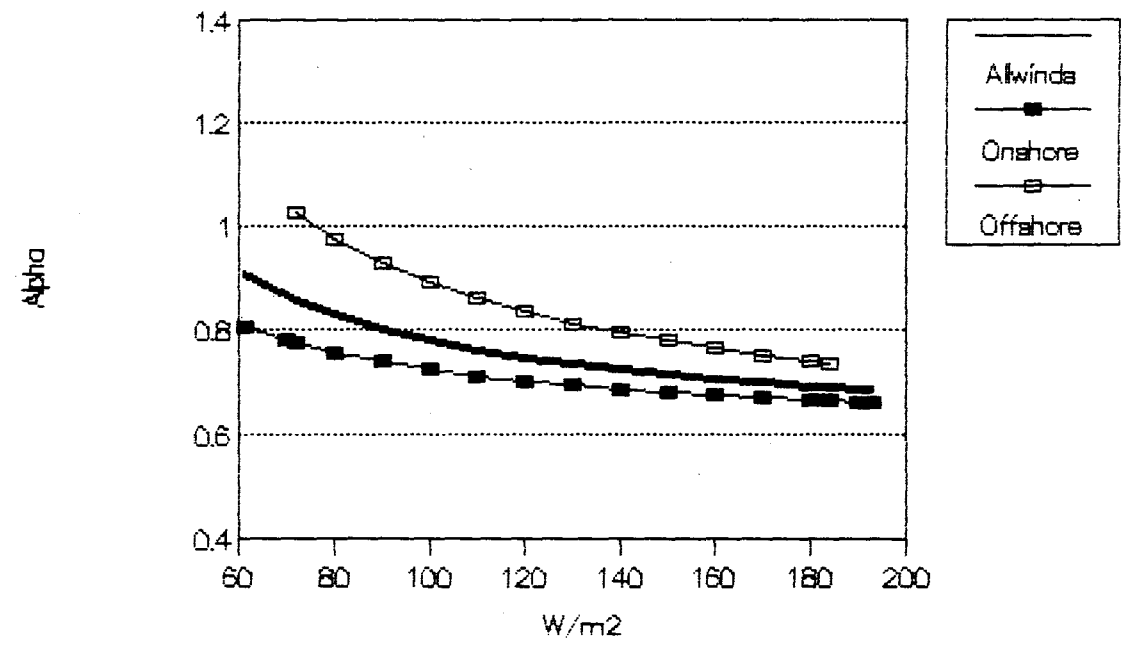

Figure 8. Sensitivity of α to r_t.

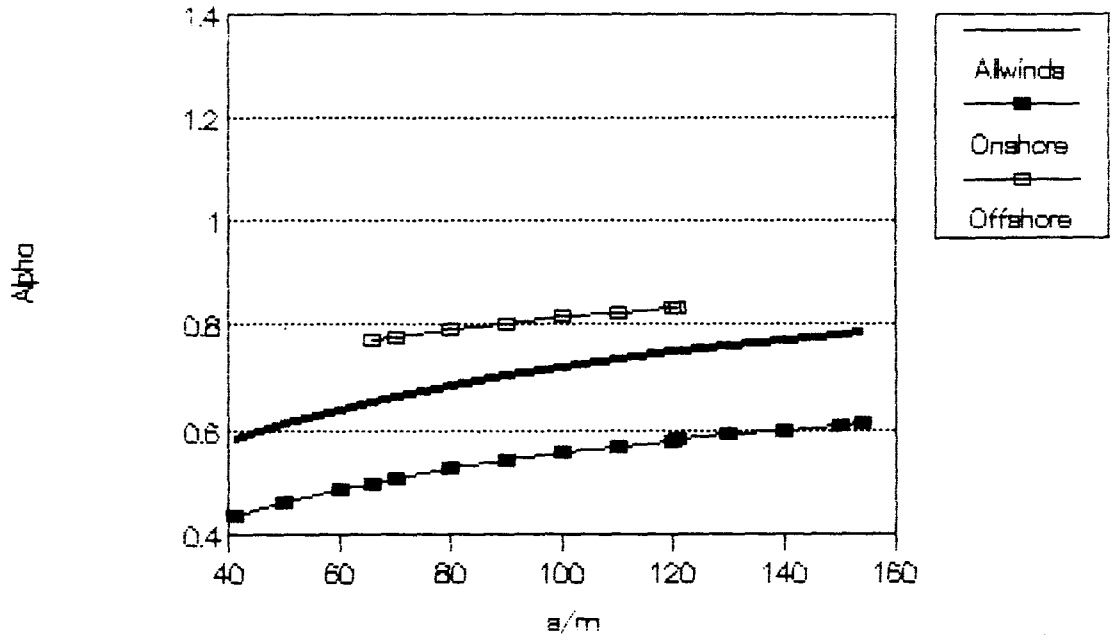

Figure 9. Relationship between wind speed and r_t.

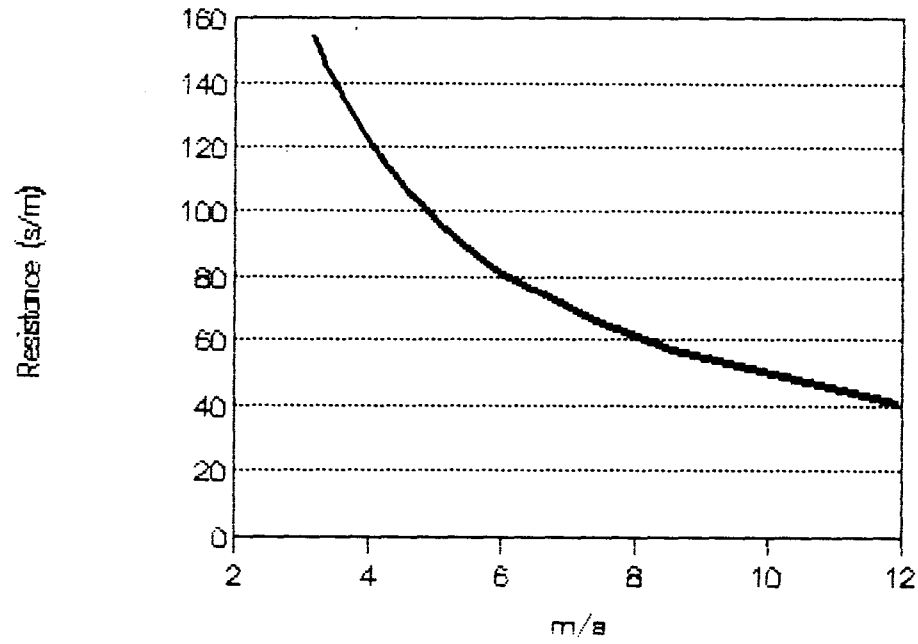

APPENDIX - SYMBOLS AND ABBREVIATIONS

Symbol	Definition	Units
Alb	Surface albedo	-
Cp	Specific heat of air at constant temperature	$Jkg^{-1}K^{-1}$
C.V.	Coefficient of variation	-
D	Zero-plane displacement	m
e_a	Ambient vapour pressure	$kPaK^{-1}$
e_s	Saturation vapour pressure	kPa
ET	Evapotranspiration	mm
k	von Karmen's constant	-
Ku	Reflected solar radiation	Wm^{-2}
Kd	Incoming solar radiation	Wm^{-2}
LAI	Leaf area index	-
P	Precipitation	mm
Q*	Net all wave radiation	Wm^{-2}
Qe	Latent heat flux	Wm^{-2}
Qg	Subsurface heat flux	Wm^{-2}
Qh	Sensible heat flux	Wm^{-2}
S	Slope of the saturation vapour pressure versus temperature curve	$gkg^{-1}K^{-1}$
T_a	Ambient air temperature	°C
r_a	Aerodynamic resistance	sm^{-1}
r_b	Bluff body resistance	sm^{-1}
r_c	Canopy resistance	sm^{-1}
r_i	Climatological resistance	sm^{-1}
r_{st}	Bulk surface resistance	sm^{-1}
VPD	Vapour pressure deficit	kPa
u*	Frictional velocity	ms^{-1}
u	Wind speed	ms^{-1}
z	Height	m
z_0	Surface roughness length	m
α	Priestley-Taylor coefficient	-
β	Bowen ratio	-
γ	Psychrometric constant	$gkg^{-1}K^{-1}$
ρ	Density of air	kgm^{-3}